Proceedings Physics with Industry 2018

Lorentz Center Leiden, the Netherlands, 26- 30 November

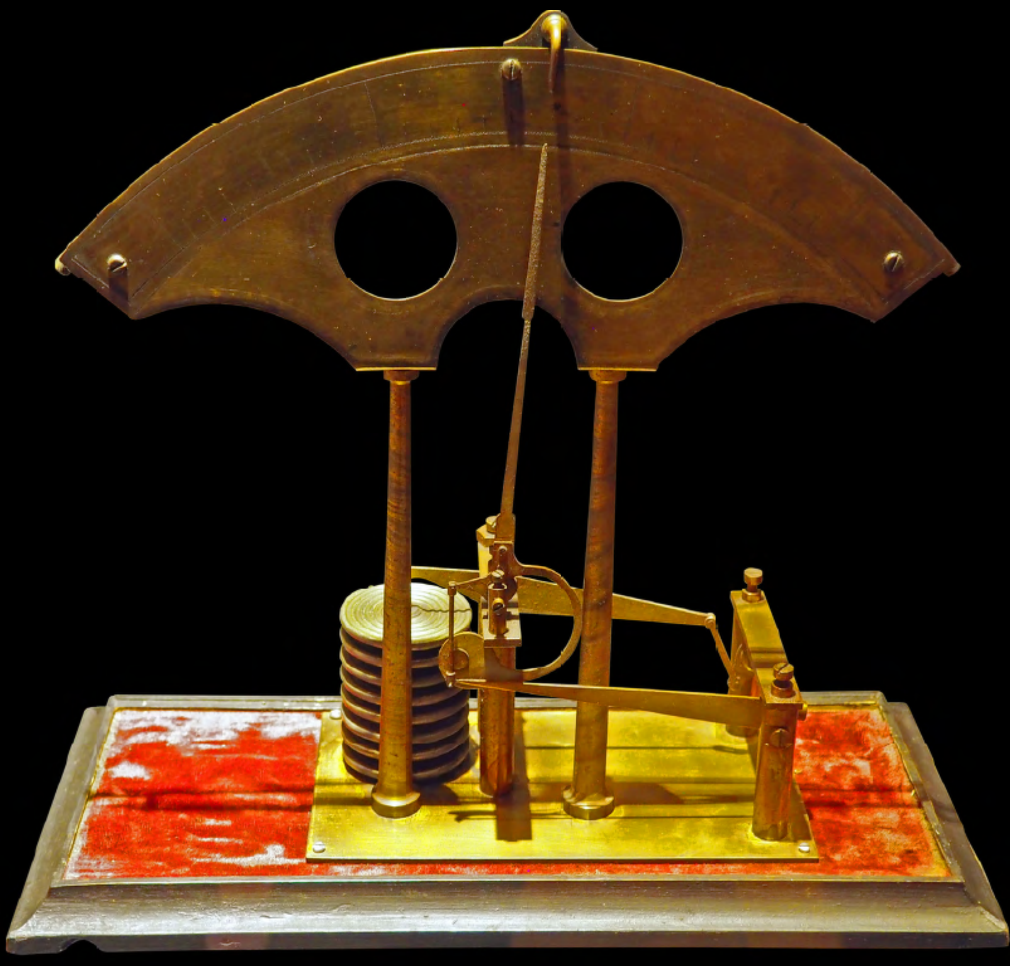

Lorentz Center Leiden, the Netherlands, 26-30 November 2018

Colophon

Text

Participants and organisation workshop.

Cover photo

Foto credit: Supernova Studio’s

Design and production

NWO, Utrecht, The Netherlands.

Thanks to

The organisation is particularly grateful for the excellent service and facilities of the Lorentz Center, the effort of the senior researchers (from the preparation phase onwards) and the enthusiastic contribution of all participants during the week. The workshop 'Physics with Industry' was organised by NWO in collaboration with the Lorentz Center. The event was funded by the Lorentz Center (which is partly funded by NWO) and the participating companies.

Table of contents

Introduction

From 26 to 30 November 2018 the ninth edition of the Physics with Industry workshop took place at the Lorentz Center in Leiden. During this week, groups of PhD students and postdocs worked together on cases provided by companies. Veco B.V., Feltest Equipment B.V., Philips and Damen delivered cases and supervision during the workshop. Besides the industrial supervision, scientific supervision was provided for each group by a senior scientist. This cooperation allowed the participant to learn about industrial problems and to work on a case outside their own academic project and the companies gained new knowledge and got innovative solutions to their problems.

Veco B.V. produces micro sieves by forming micro pores in metal through electroforming. The case that was discussed during the workshop focused on finding a solution for inaccuracies in the thickness measurements of the overgrowth and thereby allowing a better control on the pore size of the micro sieves. The participants came up with a number of solutions ranging from using a interferometer to incorporating a glass substrate and an image sensor.

Feltest Equipment B.V. joined that year with two cases. The company is a provider for tools to optimize the performance of Paper Machine Clothing. The first case focused on measuring the tension in the paper during production. Currently, the measurement results are influenced by the force on the measurement device. “Tensio+” was developed during the workshop after theoretical analysis, modelling and the construction of a prototype machine, which allows correction of the external force and results in more consistently reproducible results.
The second case was on creating an innovative sensor for the speed of the felt belts. The researchers developed “OptoSpeed”, a machine that can track the speed of the felt belts with a high speed camera.

With Philips, the researchers looked at solutions for the overheating of mobile X-ray systems, in which the X-ray tube generates too much heat for the housing. The group suggests improvements involving the X-ray generation efficiency and the heat dissipation to reduce the overheating.

Damen is involved in ship repair and relies on the quality of high tensile steel structures. Increasing the quality of the steel was the main focus of this case. The researchers identified three steps in the repair procedures, preparation of the environment, grinding and testing, and proposed improvements to optimize the process and gain a higher quality of steel repair.

The companies were grateful for all the valuable input delivered by the participants, who had the opportunity to get a look into how the industry really works.

High-Strength steel repairs – "Cutting the Edge"

Bastiaans KM[1], Caldarola M[2], Krishnamurthi S[3], Leeuwenhoek M[1,2], Liu J[4], Nafezarefi F[2], Werkman P[4]

1) *Leiden University, Leiden, the Netherlands*
2) *TU Delft, Delft, the Netherlands*
3) *UT Twente, Enschede, the Netherlands*
4) *RUG, Groningen, the Netherlands*

Academic supervisor: Richardson I, *TU Delft, Delft, the Netherlands*

Industrial partner: Kromhout K, *Damen Shiprepair Amsterdam*

Abstract

We present some ideas to improve the reliability and speed of the repair process for high strength steel undertaken in the DAMEN shipyard. This repair process consists of several steps that include preparation, welding and inspection of the material. We identified specific points in this procedure that can be improved to add reliability and to save time. We suggest simple solutions that will save the company time and cost.

Problem description

Damen Shiprepair Amsterdam would like to improve the quality of repairs on high tensile steel structures. Steel with high yield strength (>690 MPa) is used in offshore jack-ups due to its high strength and low weight, which reduces the costs while maintaining good welding properties. Due to extensive use in the energy sector, wear and tear has a huge influence of the steel structures, resulting in the need for periodic repair and limiting their lifetimes. Damen Ship repair has several years of experience in this task. However, the main challenges are to improve the repair process, increase the reliability and prevent setbacks in the process, considering all the constraints and boundary conditions. In a nutshell, the repair process has several steps: preparation of the welding environment, grinding to remove damaged material, pre-heating of the repair zone, welding, cooling down, grinding off excess material from the weld, non-destructive testing and final inspection. In total the procedure takes at least nine days, and any failure along the chain results in a return to start of the repair process. Thus, any improvement to any of these individual steps, making them faster and more reliable results in saving the company and their customer's money and time.

Solution

We identified three specific steps in repair procedure where we suggest improvements that will optimize the repair process. The first step we suggest improving is the preparation of the welding environment. Another step we found room for improvement is the grinding, which is done mechanically to remove damaged material in the beginning and excess material after the welding. Finally, we found that the non-destructive testing procedures can be improved to ensure the good quality of the weld and for early detection of defects and cracks.

A. Preparation of the repair environment

As preparation, a workable repair environment is set up using scaffolding and tent sheets. A habitat is created around the S690 structure to ensure a dry and safe environment. Setting up takes about 2-3 days for a single jack-up rig, a significant part of the 9 days total repair procedure. We recommend a faster and better way for setting up this environment:

A1) We advise to use an inflatable tent for setting up the repair environment around the S690 structure. The advantage of this method is twofold. First, setting up is fast and independent on the weather conditions. Second, the environmental conditions for the work can be controlled in a more accurate manner, providing a more robust repairing process. The main reason for this improve comes from the fact that the air inside the inflatable tent forms an insulating layer around the working environment, making the conditions more stable and easier to control.

B. Grinding (initial and final)

Grinding is one of the important elements in the repair process of S690 steel and has to be done at multiple steps in the nine-day total procedure. The initial grinding step is performed to remove damaged steel areas. A second step is used to remove excess steel that is introduced during the welding. In both situations the operator is tempted to speed up the process under time pressure. This can occur by exerting increasingly high forces on the grinding tool, thereby locally (over)heating the steel, followed by rapid and uncontrolled cool down which may create or grow cracks in the material. In addition, above this threshold temperature results in irreversible changes to the material, making it more susceptible to cracks.

We advise to improve the grinding procedure on the following points as motivated individually:

B1) We advise to provide the grinding staff with real-time, visual feedback from the temperature sensing that is already in place. The staff needs to be alerted when the temperature increase induced by the grinding approaches the upper temperature limit. This can be implemented by predicting the future temperature trajectory using a simple feedback system to warn the grinding staff. For example, we propose to use a simple visual sign like a traffic light. The visual feedback we propose is a reliable, easy-to-implement, cheap solution that can prevent local overheating of the steel.

B2) To prevent grinding-induced local overheating, cooling of the grinding surface is strongly advised. Common cooling solutions such as cooling lubricants and wet grinding are inappropriate for this task. Liquids or lubricants result in an untidy or dirty working environment, and additional cleaning steps are necessary to avoid interference with the welding procedure.

Cryogenic cooling of the grinding surface of high-strength steel is one recent academic development tested in a lab environment, showing significant improvements over dry grinding. [1] We recommend speedy implementation into the DAMEN repair toolbox. Cryogenic cooling exploits a steady flow of ultra-cold nitrogen gas coming from a liquid nitrogen tank that cools both the grinding surface and the grinding disk (as illustrated in figure 1). The temperature of the steel can be held around 200 ºC over long periods of time compared to 700 ºC without cooling, a 71% reduction of the surface temperature. This results in a smaller surface roughness (-59%) and the need of ~35% less grinding forces to remove the same amount of material per time unit. [1].

The main challenge is implementing the technique into the real working environment in a safe and user-friendly way. We identify two main risks and advise possible solutions:

B3) Handling of cryogenic liquid. Staff need basic training for use of cryogenic liquids, which can be quick (~1 day) and is cost-effective. Also we recommend double walled, vacuum insulated stainless steel tubes for the transport of the nitrogen gas/liquid, which are commercially available, robust and do not get cold on the outside.

B4) Risk of suffocation through insufficient ventilation. Cryogenic liquids/ gasses should not be used in closed environments and appropriate ventilation needs to be in place.

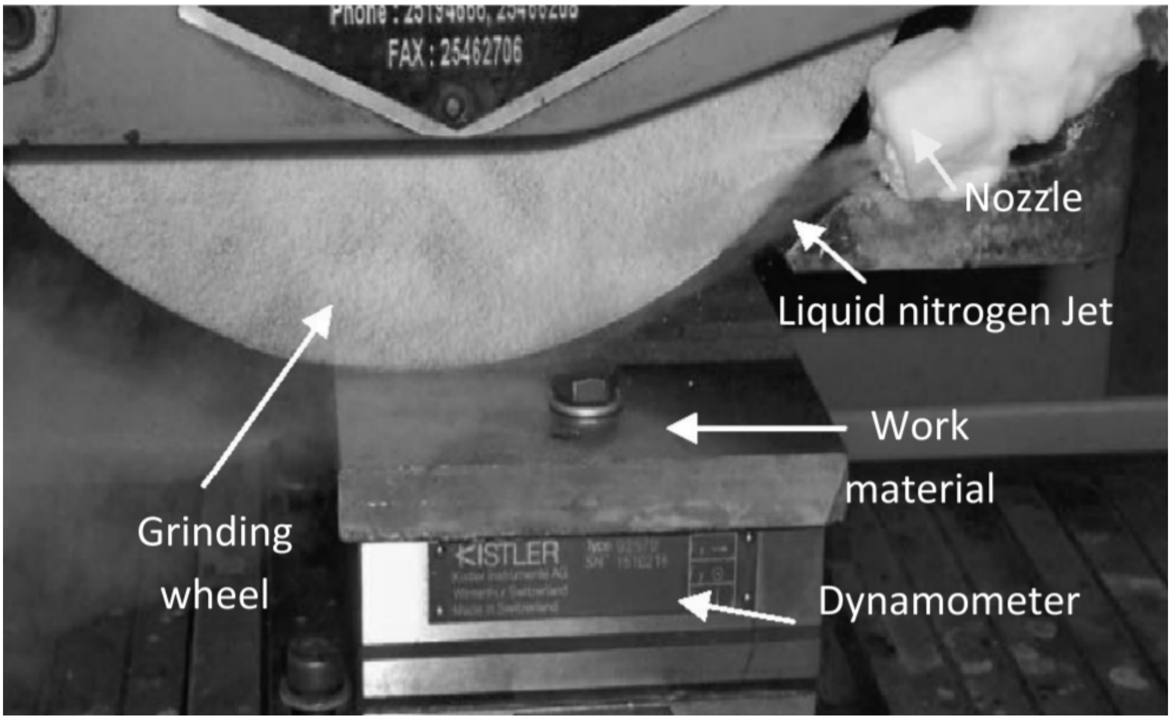

Figure 1: Experimental setup for cryogenic cooling of the grinding surface.

C. Non-destructive test: ultrasonic testing

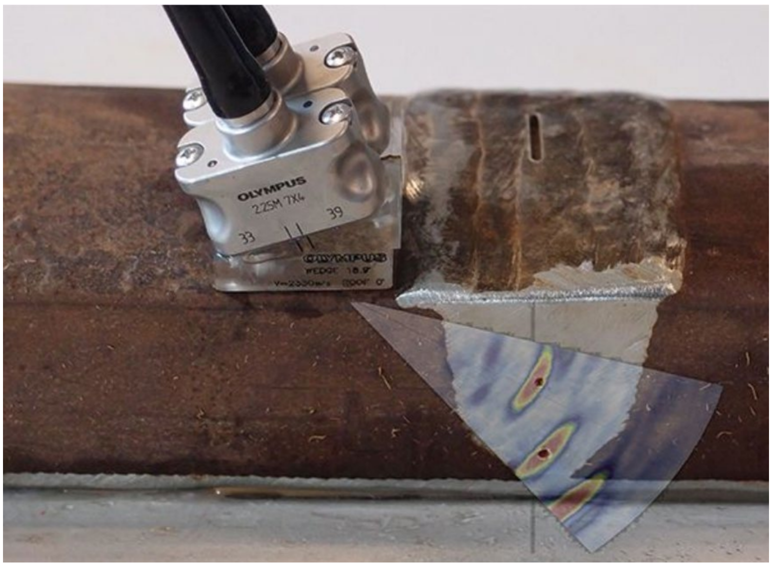

Figure 2: Ultrasonic testing to find welding cracks

Cracks –both surface and subsurface fissures - need to be identified early in the repair process, so that the damaged portion can be ground out and welded with new material. When not done perfectly, the cracks can propagate during the heating and cooling at the later stages of the repair leading to the whole process being repeated. Surface cracks can be identified by magnetic particle testing or visual inspection. However, detecting cracks that lie deep in the material is challenging. In materials with complex geometry like the teeth on the jack up rig that offer limited accessibility, non-destructive testing (NDT) analysis is complicated.

Ultrasonic testing is one way to probe deep into material and can be performed in-situ. The technique utilizes ultrasonic waves produced by a transducer (piezo-electric crystal). These are sent into the material, discontinuities such as cracks and other defects in the material reflect the incident beam back to the transducer, which also acts as the receiver, based on the time delay and amplitude of the signal, the discontinuities can be located. [2] Phased array is an advanced method that uses multiple transducers that can be pulsed sequentially and the time delays from the reflected wave front contains information about defects in the material (Fig. 2). There are many advantages to this technique such as, rapid inspection and minimal operator training requirements. [2].

The issues of ultrasonic NDT are not limited to complicated external geometry. Another difficulty is the detection of cracks in welds. At the typical wavelength of ultrasound used in practice, the parent material can be modelled, to a very good approximation, as isotropic and homogeneous. This approximation works especially well in fine-grain steels such as S690. However, in the fusion zone of a weld, grain boundaries orient themselves along a preferred direction. The anisotropy has important effects for the propagation of pressure waves through the material. The grain size in the material also becomes larger and larger as one moves from the heat-affected zone to the fusion zone.

An important effect induced by anisotropy is beam steering. [3] An ultrasound beam traveling through a weld will follow a curved trajectory defined by the local orientation of grain boundaries. This has consequences for the detection of defects in this area of the material. An important technique used in weld inspection is the focusing of ultrasound. A phased array is capable of focusing the energy in a pulse to a particular location. Each element of the phased array sends approximately spherical waves of ultrasound into the material. The total wavefront, to a very good approximation, is the sum of the individual spherical waves sent out by the piezo-electric elements. By sending out the waves with very specific time delays between the piezo-electric elements, it is possible to concentrate the energy in the ultrasonic pulse to a small region by constructive interference. The effect of beam steering, however, spoils the focusing and spreads the energy around, making it difficult to transfer enough power to the point of interest. It is possible to account for the effect of beam steering in controlled situations, therefor we recommend:

C1) By varying the time delays between elements of the phased array from the values they take in an isotropic medium, one can compensate for beam steering. [4] This can have dramatic effects for the power transmitted to the point of interest.

C2) We propose a method to make this technique insensitive to the precise details of grain distributions in the material. By varying the time delays between elements it should be possible to compensate for beam steering even without precise knowledge of the actual distribution. When one finds an enhanced signal for a choice of input parameters, the pulse energy is focused on a feature of the material. The problem is that it is hard to know exactly where the beam is focusing without an understanding of how ultrasound propagates through the weld area. A large signal could correspond to a reflection off a material defect, the boundary of the material or an interface between media.

C3) We propose to use two different frequencies to probe the material. A low frequency scan probes the geometry of the boundary and material interfaces, but does not see small defects. By varying the steering parameters until one detects an enhanced signal, one compensates for the effect of beam steering. Then, a high frequency scan probes for material defects. An important aspect to understand is the frequency dependence of the beam steering effect. This technique should allow to focus the energy of a phased array by the method of reference [4] even without detailed understanding of the propagation of ultrasound in the material. It will be necessary to understand the frequency dependence of the beam steering effect. This requires either experimental knowledge or modelling of how the refractive indices change along the weld and how they change with frequency.

A recent academic improvement on phased array transducers are flexible transducer probes, these might provide significant advantages in the further future:

C4) Phased array with a flexible probe, a recent development that uses piezoelectric composites as transducers, is a promising new technique that possibly can be applied to nonplanar complex surfaces in the future(Fig. 3). This design enhances the level of device integration compared to single transducer designs. It might be more applicable for the teeth on the jack [2], as it can be seen from the example in figure 4.

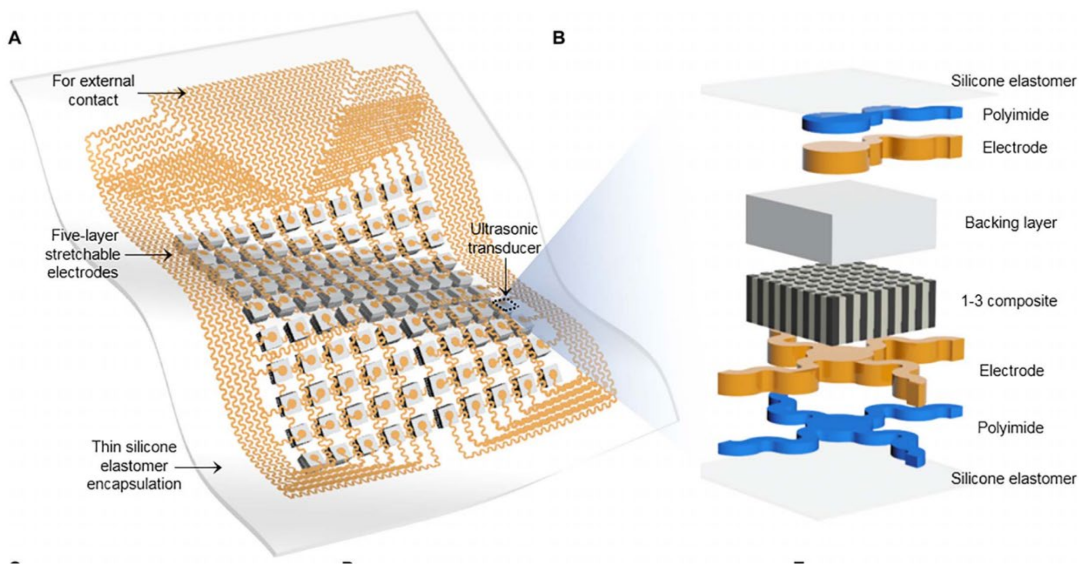

Figure 3: Schematics of a flexible ultrasonic phase array. (A) the device structure. (B) detailed structure.

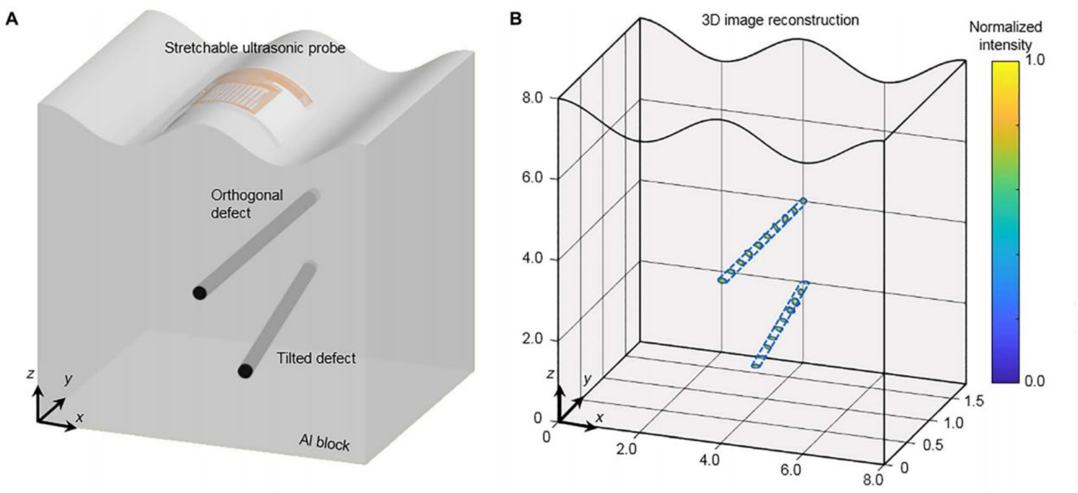

Figure 4: 3D image reconstruction illustrating the location of defects.

References

[1] G. Manimaran *et al.* Cryogenic **59**, 76-83 (2014)

[2] H. Hu *et al.* Science Advances **4**, eaar3979 (2018)

[3] G.D. Connolly, PhD thesis, Imperial College London (2009)

[4] H-H. Kim *et al.* Nuclear Engineering and Technology **48**, 228- 235 (2016)

Feltest OptoSpeed

Mina Morshed Behbahani[1], Annemarie Berkhout[2], Thomas Jollans[3], Vincenzo Mascoli[4], Chris Ripken[5], Nasim Tavakoli[2] & Martijn Tros[4]

[1] *University of Groningen, Groningen, The Netherlands*
[2] *AMOLF, Amsterdam, The Netherlands*
[3] *Leiden University, Leiden, The Netherlands*
[4] *Free University Amsterdam, , Amsterdam, The Netherlands*
[5] *Radboud University, Nijmegen, The Netherlands*

Academic supervision: Dr. Herman Offerhaus, *University of Twente, Twente, The Netherlands*
Company: Feltest Equipment BV, Eerbeek
Contact persons:
Marcel Lensvelt
Wim Stenfert Kroese

Problem description

Feltest is a small company which aims to develop new tools to support and improve paper mills and the paper production industry. For the workshop Physics with Industry, organized by the Dutch Organization for Scientific Research (NWO), they posed the challenge to come with a design of a felt velocity measuring device.
Paper is produced on machines that employ several hundreds of meters of belt, made of felt. In order to optimize the production process, it is key that the speed of each belt is exactly known. Designing an innovative sensor for the speed of felt belts is the main assignment for this workshop.

The sensor should meet the following requirements: A paper mill is a large and expensive machine, and every mill is different. Therefore, no changes can be made to the machine, and the sensor needs to operate for the different types of mill. Furthermore, paper mills operate continuously, so the device needs to work on a running machine. The felts in the mill run typically with ~36 m/s (130 km/h), so for safety reasons the employee needs to be able to measure the speed without touching the belt (contactless). Finally, it should be possible to measure the velocity of several felts in different parts of the mill (for instance at the beginning and the end), meaning the velocity sensor needs to be hand-held. This also means the operator must be able to measure the velocity from every possible angle and distance of the felt. Finally, the sensor should be as precise as possible, preferably below percent-level accuracy.

Solution

As a solution, we propose a device that measures the speed by means of a high speed camera. At the workshop, we built a prototype to demonstrate that the principles of our solution are feasible. See figure 1.

Figure 1. *Prototype built during the workshop.*

The solution is based on the tracking of a recognizable feature on the belt. Each belt is closed at a seam, recognizable as a black line. This can be recorded with the camera. To determine the velocity of the black line, the camera should have a sufficiently fast frame rate. It should be able to at least record two frames before the seam leaves the field of view, with which the speed can be calculated from the displacement of the marking. Our prototype has shown that this is almost feasible for a standard commercial camera. In order to achieve optimal result, for a velocity of 36 m/s a typical frame rate of about 100 fps is needed. This is a speed easily reached by modern commercial (~2000 euro) high speed cameras (500 to 1000 fps).
The position of the sensor operator with respect to the felt (angle and distance) is variable. However, using the camera we can only determine displacements parallel to the camera lens. Thus, we also have to determine the relative orientation of the belt with respect to the camera. Our prototype uses four laser distance meters in a square geometry pointing parallel to each other and the camera. With these points as a reference in the image, the angle of the camera to the felt and therefore the direction of the moving belt in 3D with respect to the 2D camera image can bedetermined.
We have developed a coordinate transformation algorithm that takes care of corrections due to motion in the direction of the camera. With the interframe timing being known accurately, the displacement of the belt's seam in subsequent frames can be calculated. For this, we have implemented a cross correlation or phase correlation, subtracted by the mean autocorrelation. Our prototype achieved encouraging results in determining the corrected displacement.
There are several aspects important to the accuracy of the velocity measurement. Firstly, the contrast of the black line is vital. important factors here are sufficient light in a small exposure time, a high resolution that is dependent on amount of pixels as well as the magnification (focussing) and the frame rate of the camera. Furthermore, motion of the operator and device has to be considered, which include vibrations (from the operator or the mill) and small translations (by the operators hands). Various technical solutions (tripods, stabilizing hardware/software) are available to keep these sources of error to a minimum.

Conclusion

In conclusion, the prototype provides a basic implementation for determining the speed of the felt, from data acquisition to processing. We have shown achievability of the concept for each stage, and provided suggestions for improvements.

The Physics with Industry workshop was an excellent opportunity for an interdisciplinary collaboration. Our group consisted of physicists with very different background, ranging from biophysics to theoretical quantum gravity. Nevertheless, the workshop's format is set up in such a way that everyone's expertise can be put to use. Starting with an open-minded brainstorm session, every possible solution can be explored. Furthermore, the workshop also allows for building a prototype in the timespan of just a few days.

Tensio+: a fabric tension meter for the paper industry

Pepijn Beekman[1], Fausto Casburo[2], Christos Messinis[3,4], Amin Moradi[5], Melissa Piontek[6], Cameron Price[7], Tom van der Reep[5] and Martin de Wit[5]

[1] Laboratory of Organic Chemistry, Wageningen University, 6700 EG Wageningen, The Netherlands
[2] "La Sapienza" University - Physics Department and "National Institute of Nuclear Physics (INFN)" , P.le A. Moro 5, 00185 Roma, Italy
[3] Department of Physics and Astronomy, and LaserLaB, Vrije Universiteit, De Boelelaan 1081, 1081 HV Amsterdam, The Netherlands
[4] Advanced Research Center for Nanolithography (ARCNL), Science Park 110, 1098 XG Amsterdam, The Netherlands
[5] Leiden Institute of Physics, Leiden University, Niels Bohrweg 2, 2333 CA Leiden, The Netherlands
[6] Molecular Biophysics, Zernike Institute for Advanced Materials, University of Groningen, 9747 AG Groningen, The Netherlands
[7] Instituut Lorentz, Universiteit Leiden, P.O. Box 9506, 2300 RA Leiden, The Netherlands

Academic supervision: Dr. Hans Goosen, TU Delft, Delft, The Netherlands

Company: Feltest Equipment BV, Eerbeek
Contact persons:
Marcel Lensvelt
Wim Stenfert Kroese

Problem description

Paper is produced in vast quantities in paper mills. The properties of the produced paper critically depend on the parameters of the mill, especially the properties of the fabric belt transporting the fibre-water mixture that is converted into paper through the mill. The belt properties are currently monitored by indirect methods and imprecise measurement devices. The company Feltest Equipment BV aims to improve this situation by developing measurement equipment to monitor the belt properties in a direct fashion.

During the workshop *Physics with Industry 2018* we considered the measurement of the tension in the fabric. At the moment, the fabric tension is measured using a single load cell. This makes the measurement operator dependent as the measurement result is influenced to a great extent by the force that the operator exerts on the measurement device. To this end, Feltest Equipment BV developed a device incorporating multiple load cells in order to correct for the operator's influence on the measurement result in a consistent reproducible manner.

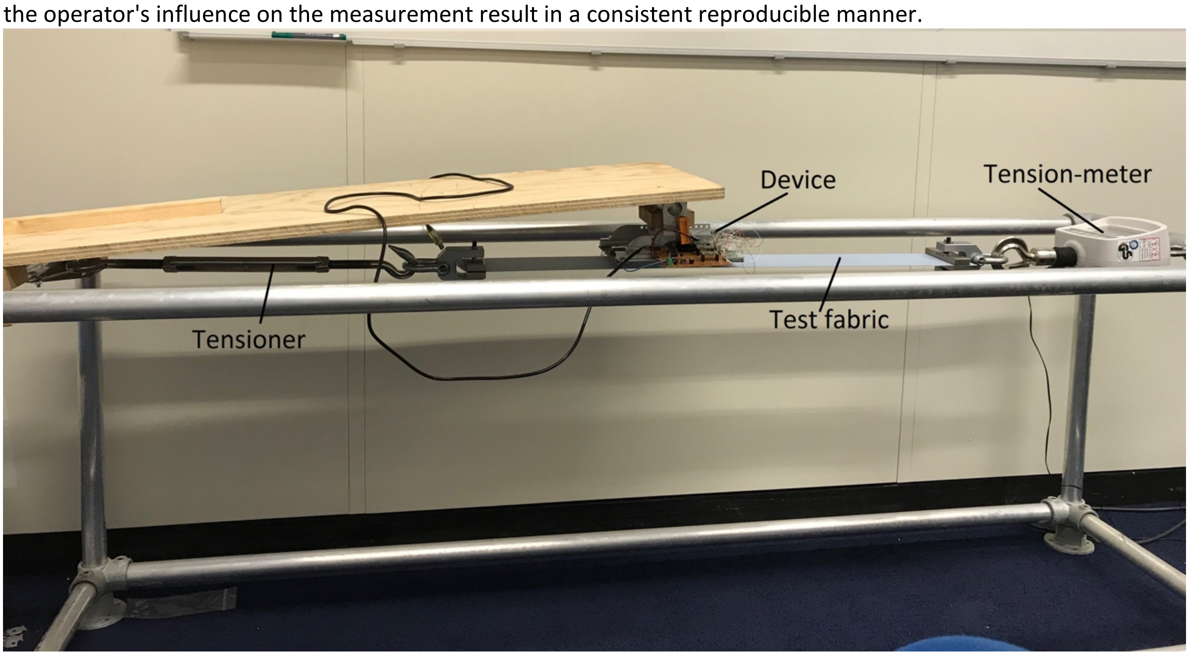

Figure 1: Test set-up. Indicated are the device, the test fabric, the tensioner and the tension-meter.

Solution

During the workshop our group tried to tackle this challenge with a threefold approach. First, we studied the problem theoretically using a simplified analytical model. Secondly, the problem is modelled using numeric methods and thirdly we are provided with a prototype of the device and a test set-up in order to perform experiments, see figure 1.

Within the analytical analysis, we modelled the device and fabric as a 2D-system. From this model we obtained expressions of the forces measured by the device as function of tension and a model of an operator assuming the device and fabric are in equilibrium and friction-less. However, comparison between theoretical and experimental data showed that our model failed to capture the full detail of the experimental situation adequately.

For the numerical analysis, the fabric was modelled as a 2D-sheet in Comsol and its behaviour under point indentation was studied. From this analysis we found that the indentation should not depend on the operator force along the width of the fabric (perpendicular to direction of motion of the fabric), whereas it mildly depends on the operator force along the length of the sheet (parallel to the direction of motion). However, since the sheet approach leaves out many physical effects and the fact that the fabric in the experimental set-up is slender, we could not test whether these predictions hold in an experimental environment.

Finally, we gave suggestions for possible improvement of the device given our analysis.

Overheating of mobile X-Ray systems

Yuqiang Gao,[a] Julia Krug,[b] Christie Nguyen,[c] Rohit Sasidharan Nair,[a] Nico Schmidt,[d] Cristina Sfiligoj[e] and Amitesh Singh[f]
a. University of Twente, b. Wageningen University, c. Single Quantum BV, d. University of Groningen, e. ARCNL,
f. Leiden University, AMOLF

Gerard van Rooij[g]
g. DIFFER

Bas Feddes,[h] Hans Roberts[h] and Hans Rosink[h]
h. Philips Healthcare

Abstract

Overheating of mobile x-ray systems is a problem during long complicated surgery procedures. This is caused by the X-ray tube generating more heat than the housing can dissipate. Two options for improvement include increasing of X-ray generation efficiency increasing the heat dissipation of the system. We specifically present a solution for increasing the heat dissipation for a short-term improvement, while we briefly mention some ideas and approaches for improvements on the longer term.

Context and System Description

Philips healthcare is providing a vast variety of imaging systems to hospitals and medical centres. In the image-guided therapy unit, mobile X-ray systems (Figure 1) are developed to enable the flexible use of imaging for a manifold for different treatments in the operating room. The movable C-arm system enables the orientation and versatility of use. They can be moved between different operating rooms which allow the flexible use of the system in an operating room as compared to fixed systems in diagnostics. Mobile systems enable live imaging during complicated surgery studies. Components of the system are the X-ray tube with a rotating anode immersed in an oil bath for heat dissipation and a detector on the other side of the C-arc.

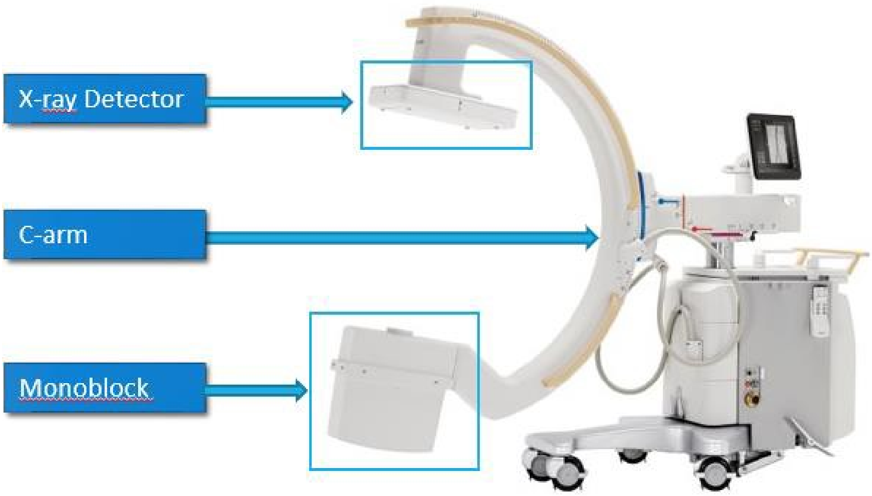

Figure 1. A typical Philips Mobile X-ray system with a C-arm, an X-ray detector and a monoblock containing the X-ray generating tube is depicted.

Problem description: Overheating of the system

Complicated procedures that require live imaging (e.g. catheterization studies) involve continuous operation at high image quality and resolution. Therefore, the X-ray tube is operated continuously at high power. The anode reaches temperatures up to 1000 °C in this process and subsequently heats the oil bath which has a maximum temperature allowance at 60 °C. Once the oil bath reaches this maximum temperature, imaging is disabled, and the operation must inevitably stop to allow the oil bath to cool down for at least 45 minutes. During this time the emergency mode with a low x-ray dose is available only for e.g. catheter removal. From a physical point of view this means that heat generated by the X-ray tube during X-ray generation exceeds the heat which is being dissipated by the system as shown in Figure 2.

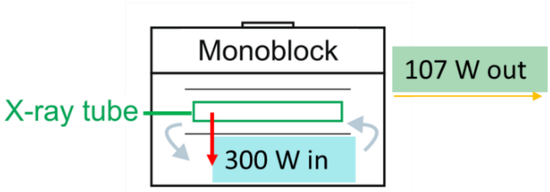

Figure 2. The monoblock of the C-arc contains the X-ray tube and the oil bath.

The desired scenario for an improved system was set to enable a scenario in which the mobile X-ray system can be used for 3 surgeries with each a 3-hour duration and a 30-minute break in between surgeries. The X- ray tube will operate at 300 W during this time.

Several constraints need to be considered when assessing possible solutions. First, the mobile system is used in a clinical setting, hence in a sterile environment. Second, mobility of the systems means that weight, size and stability are crucial aspects. The solution for improvement must be user-friendly and should involve as little maintenance as possible. Furthermore, it must comply to regulations posed by health authorities. From an X-ray physics point of view, the focal spot should be as small as possible. Costs and marketing aspects of the solution play a role in this industry case. As general guideline, all possible solutions were considered in light of the impact they achieve with respect to the problem and the time frame needed for R&D to implement the solution.

Approach to problem solving

There are two general approaches: Either decreasing the amount of heat generated by the X-ray tube or to improve the amount of heat that can be dissipated by the system.

X-ray generation is very inefficient. While only 0.9% of the energy input is converted into the X-ray generation, a fraction as low as 0.03% of these generated X-rays reach the target area which is examined. Decreasing the amount of heat generation by X-ray for a more efficient X-ray generation could be achieved by either increasing the overall yield of X-ray generation or to improve the number of X-rays which reach the sample, i.e. increasing the solid angle.

The Stefan-Boltzmann equation below shows that we can improve the heat dissipation by either increasing the area of the surface and the temperature difference of the two compartments:

$$Q = \sigma A({T_b}^4 - {T_a}^4)$$

Here, Q is the radiative heat transfer from a black body of surface area A at temperature T_b in an environment at temperature T_a.

X-ray generation and X-ray Optics

To review the possibilities for improving X-ray generation and focussing we have briefly looked at the latest research towards anode and cathode improvement as well as the latest X-ray optics for an improvement of the solid angle of X-rays reaching the target.

The rotating anode X-ray tube has not changed fundamentally over the last 90 years. The principle is based on heating a filament and eject electrons by thermionic emission and accelerate them towards the anode. Alternative cathodes were proposed which eject electrons via field emission. Carbon Nanotube (CNT)- based cathodes are one example of these field emission cathodes under examination[1,2] with the advantages being a more controlled electron beam and lower power consumption[2]. While the focal spot size with thermionic cathodes is in principle defined by the size of the filament and is reduced by additional focussing of the electron beam, carbon nanotube cathodes currently reach smaller focal spot sizes[2] than the current X-ray tube based on thermionic emission used by Philips. However, these CNT-cathodes are still facing stability and fabrication difficulties and are currently being projected to be commercially competitive with conventional X-ray anodes in approximately 10 years[2].Focusing the X-ray beam onto the patient using X-ray optics can possibly reduce the operational power required for the surgery while also minimizing the heating. Since we are dealing exclusively with High Energy X-rays with energy > 40keV, we have limited options (as opposed to soft X-rays). Let's look at the three ways to manipulate electromagnetic radiation: Refraction, Reflection and Diffraction.[4,5]

1. Lenses: Refractive index for almost all materials is practically 1 when exposed to X-rays. The range varies from 1 to $1\text{-}10^{-5}$ for soft X rays, which is reduced further in the case of Hard X- rays. Compound refractive lenses for X-rays made using Aluminium were demonstrated in 1995 for the first time. While it is theoretically complex in the first place, practical considerations make this idea impossible to execute. The radius of curvature of such lenses is under a millimetre making the lenses too small for our purpose and it takes 10^2-10^3 lenses to achieve substantial focusing. Having a wide 2D array of tiny lenses stacked on top of each other in the order of hundreds does not meet our space, weight and economic constraints.

2. Mirrors: Grazing angle reflection of soft X-rays has been demonstrated using setups like Wolter telescope and Kirkpatrick-Baez reflective microscope using reflective materials such as Gold and Iridium. Since this is only a grazing angle reflection, only a narrow beam of X-rays can be reflected making the benefit incremental (and not substantial). Moreover, for hard X- rays, such systems have only been manufactured for applications like space telescopes which probably makes this solution too expensive. It is important to mention that a delicate and expensive mirror system inside the monoblock is bound to destroy the robustness of the system which is designed for rough use in hospitals.

3. Zone Plates: Diffraction is promising given that one does not deal with thick compound lenses or delicate mirrors, but with thin robust zone plates. Such plates have proven useful for soft X-rays on a small-scale systems. However, for hard X-rays, one has to look towards alternatives like Multilayer zone plates and Laue lenses. Although these have been demonstrated in research to work on X-ray energies up to 100 keV, there is no commercial availability rendering the solution unviable at this stage.

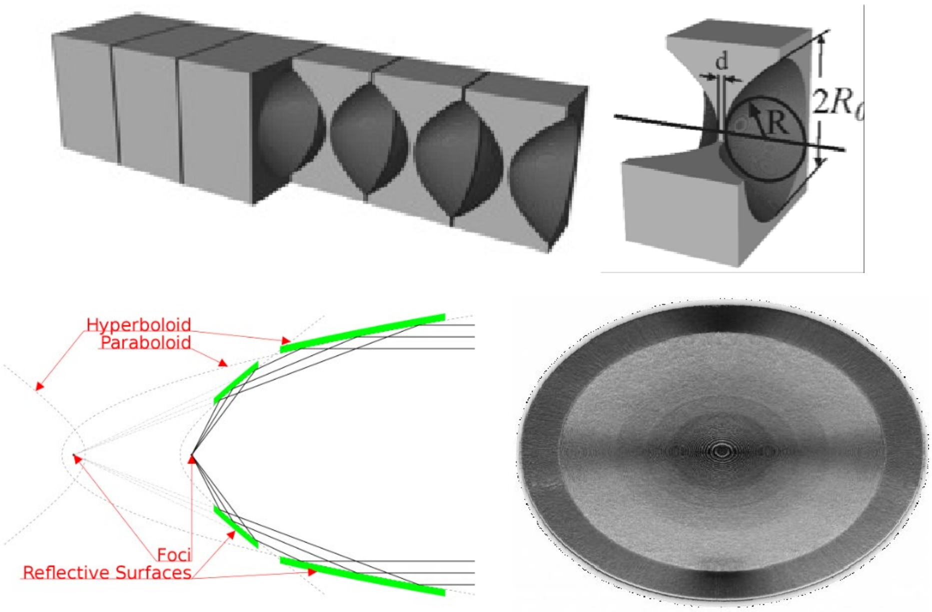

Figure 3: Compound Refractive Lenses (CRL) for X-rays (Top)[6], Wolter telescope Type 1 (Bottom left)[7] and Commercially available Fresnel Zone Plates for Soft X-rays (Bottom right)[8]

Improving the heat dissipation

Operation time of the X-ray device can be extended by keeping it under safe temperature limits for a longer duration. This can be achieved by active and passive cooling. Here, we propose a passive cooling solution that does not involve external cooling circuits or devices. The core of the idea is to improve the heat dissipation by spreading the heat to a larger area which is already available in the current design. In the current design, the external surface area of C-arm is 2.67 times the surface area of the monoblock. This implies that for an ideal case without any heat losses and assuming unit emissivity and uniform temperature for all surfaces, one can achieve 3.67 times more heat dissipation by making additional use of the C-arm (Figure 4). Here, we neglect any natural or forced convection to the ambient and radiation is considered as the dominant heat dissipation mechanism.

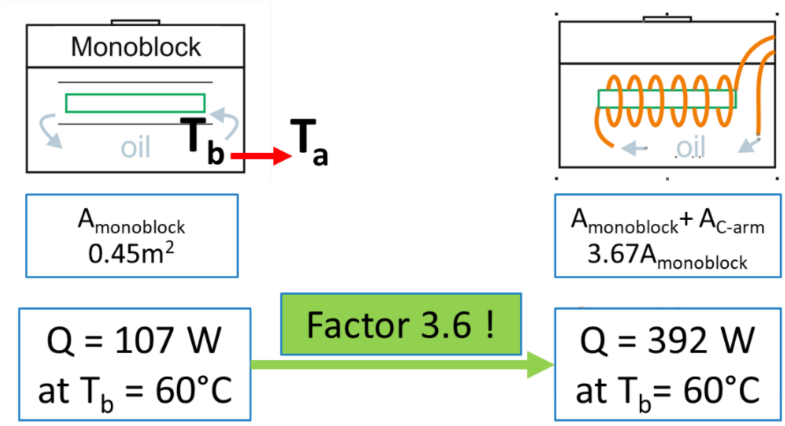

Figure 4. A comparison of heat dissipation for an ideal case by making use of C-arm for additional heat dissipation.

Figure 5 shows a schematic of the proposed design. The heat radiated from the X-ray source is removed by a shell and tube arrangement. Cold oil from the reservoir is pumped into the shell heating the oil up, the hot oil from the other end is then transported to the heat exchanger on the top plate of the mono block. Solid copper pipes run through the ducts inside the C-arm in the new design.

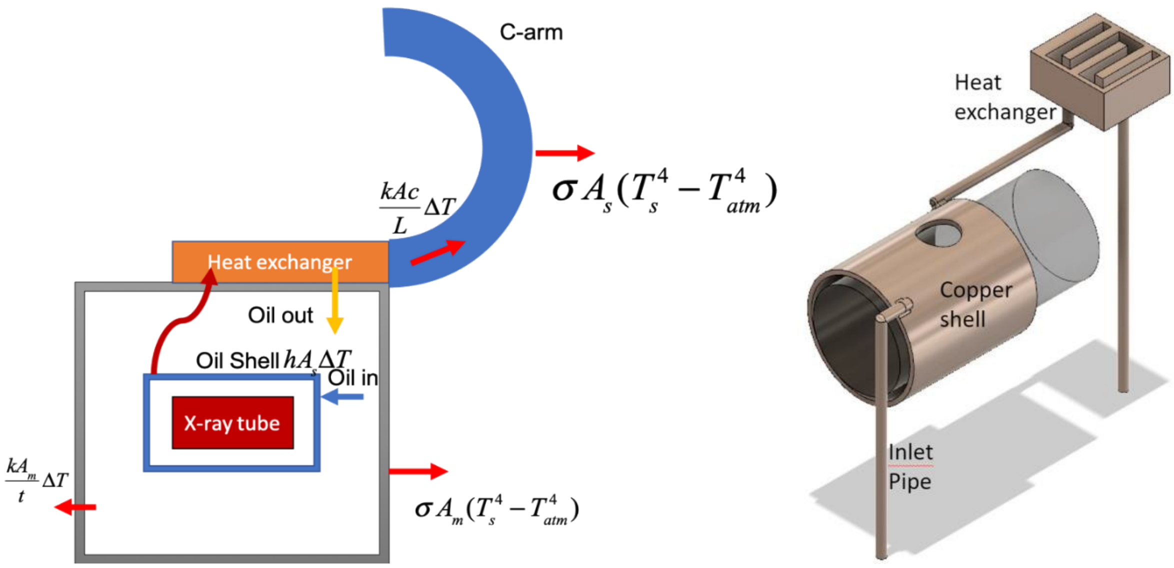

Figure 5. Schematic of the proposed design for improved heat dissipation: Block diagram (left) and implementation. (right)

The copper pipes are connected to the heat exchanger, thus conducting the heat to the top of the C- arm. One way to transfer heat between the copper pipes and the C-arm body is by radiation. The C- arm then acts as a hot body radiating heat to the colder outside ambient air. Another way to achieve heat transfer between copper pipes and the C-arm body will be through full thermal contact. In the present discussion, the mechanism of heat transfer inside the C-arm is not considered in detail for analysis rather we evaluate the performance of the entire X-ray unit and the C-arm for different values of heat exchanger efficiencies. This will allow us to engineer the heat exchanger, surface emissivity, copper pipe design etc. to achieve an effective efficiency to ensure better performance of the whole unit. We consider two cases here, one with a solid copper pipe inside the C-arm and the other with a copper heat pipe with water as the working fluid inside the C-arm.

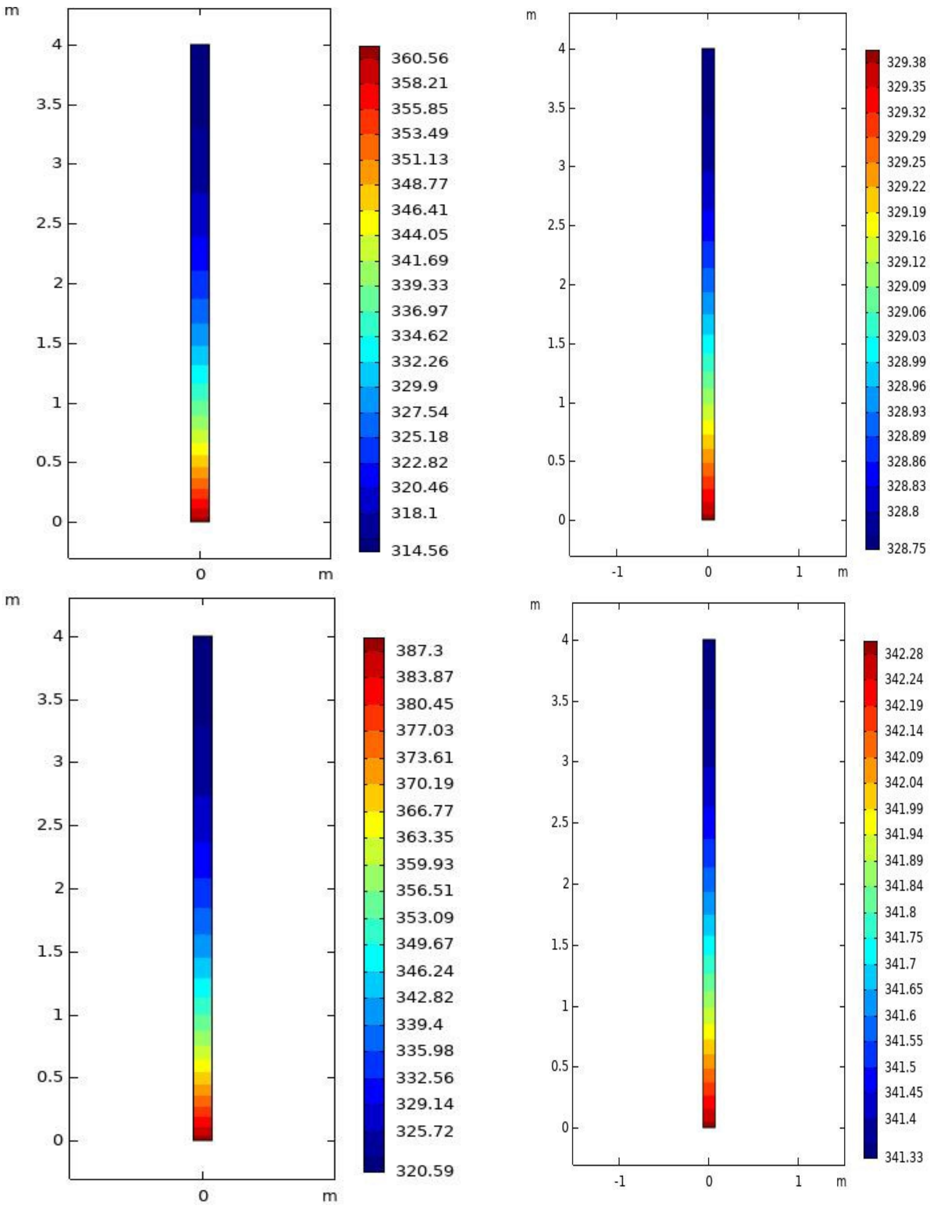

Figure 6. Temperature distribution of the C-arm with copper (left) and heat pipe(right) for 50% (top) and 75% (bottom) efficiency of the heat exchanger.

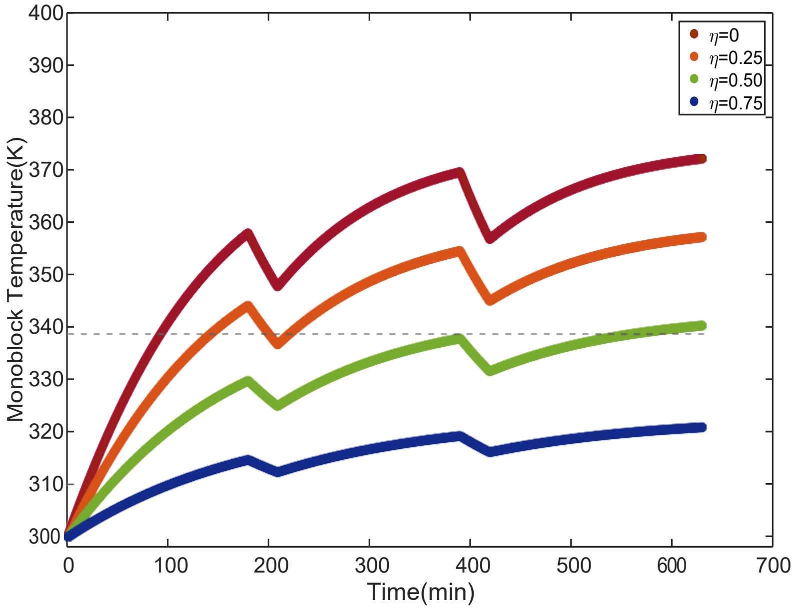

Figure 7. Transient performance of the monoblock for 9-hour operation with 30 minutes of break after every 3 hours for heat exchanger efficiencies (η) of 0, 0.25, 0.50 and 0.75.

Figure 6 shows the comparison of temperature distribution of the C-arm modelled as a 2-D rectangular rod of equivalent dimensions with copper pipes and heat-pipe. There is a hot spot above the safe limit in-case of the copper pipes. However, the average surface temperature is below the safe limit. Addition or replacement of copper pipes with heat pipes would solve the problem of the hotspot as seen in the Figure 6. One might want to consider a combination of copper pipes and heat pipes since our theoretical models are for an ideal scenario with radiation as the sole mechanism of heat dissipation to the ambient whereas in actual case other mechanisms also contribute which would result in a lower surface temperature than predicted. We also see the transient performance of the monoblock for different efficiencies of the heat exchanger at the top plate. It can be seen that the X- ray unit can operate well under the safe temperature limits for longer duration compared to the previous design (Figure 7). Considering the overprediction of the model as discussed previously, we expect the X-ray unit to perform for longer duration under the safe limits and also to be within the safe limits for heat exchanger efficiencies lower than the predicted limit of 50%.

The oil in the shell surrounding the X-ray tube is exposed to a large heat flux compared to the previous design where the entire heat was dumped into the reservoir directly. Hence, it is important to ensure that the oil is well below the critical temperature in the new design. Figure 8 shows a simple case of 2D CFD simulation for the shell with oil pumped in at 2600 ml/min which can be easily achieved by a micropump M400S. It can be seen that the maximum oil temperature is below the safe limit for 300 W heat generation at the X-ray source with a 6 mm hydraulic diameter for the oil flow.

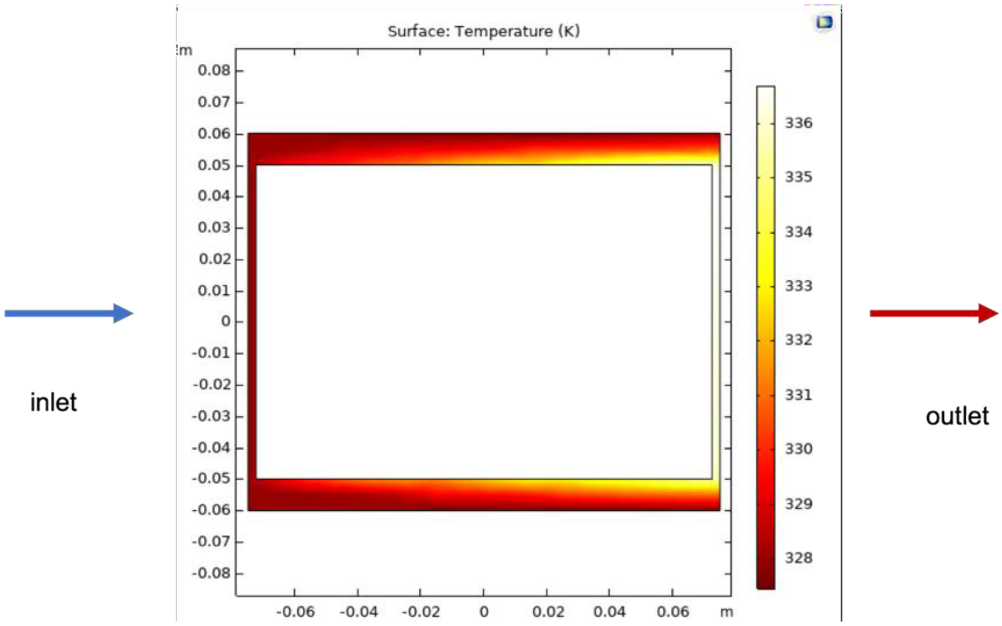

Figure 8. Temperature distribution of oil in the shell for a heat source of 300W uniformly distributed over X-ray tube surface.

Conclusion

The main goal of this workshop for Team Philips was to extend the runtime of Mobile X-ray systems during back-to-back prolonged surgeries in hospitals. The main obstacle faced by users is the partial shutdown of the system due to overheating of the monoblock. From a purely scientific perspective, this is a simple heat transfer problem. So, we started by examining all the components of the Philips Mobile X-ray system to identify areas where significant improvements could be achieved by minimal changes to the existing product design. The solution had to be economical enough to implement and could not adversely impact the robustness of the system. User-friendliness had to be maintained and marketing considerations meant that we could not reuse ideas from competing brands. Regulatory constraints and hospital safety regulations impose certain restrictions too. Lack of high-tech infrastructure in certain hospitals and a maintenance frequency of only once per year meant that pragmatic easy-to-implement solutions had be favoured over cutting-edge complex solutions.

A large majority of proposed solutions were therefore quickly discarded after initial discussions, and a subsequent deep dive eliminated many of the remaining ones. We finally focused on 2 aspects: X ray generation & focusing, and improving heat dissipation of the monoblock. The former has potential over the long term, whereas the latter offers quick fix solutions that can be implemented within the next couple of years. The team's recommendation to Philips would be to pursue both these solutions in two phases. Philips engineers can begin implementing the heat dissipation solutions immediately by adjusting the current X-ray mobile system models and roll out the improved systems over the next 5 years. Meanwhile, Philips R&D scientists can aim to develop, possibly in collaboration with academia, long-term solutions such as CNT cathodes and Multi-layer zone plates which might be the next big breakthrough in Mobile X-ray systems.

References

1. Puett, C. *et al.* An update on carbon nanotube-enabled X-ray sources for biomedical imaging. *Wiley Interdiscip. Rev. Nanomedicine Nanobiotechnology* **10,** 1–11 (2018).

2. Parmee, R. J., Collins, C. M., Milne, W. I. & Cole, M. T. X-ray generation using carbon nanotubes. *Nano Converg.* **2,** 1 (2015).

3. Incropera, F. P., & DeWitt, D. P. Fundamentals of heat and mass transfer. New York: J. Wiley (2002)

4. Schroer C., Lengeler B. X-Ray Optics. In: Träger F. (eds) Springer Handbook of Lasers and Optics. Springer Handbooks. Springer, New York, NY (2007)

5. Rubensson, J.E. Ch. 6: X-ray optics, Synchrotron Radiation: An everyday application of special relativity (2016)

6. JJ X-ray [https://www.jjxray.dk/products/refractive-optics], Accessed on 11-04-2019

7. Andreas 9384 [https://commons.wikimedia.org/wiki/File:Wolter-I_01.svg], Accessed on 11- 04-2019

8. Applied Nanotools Inc. [https://www.appliednt.com/x-ray-zone-plates/], Accessed on 11-04- 2019

In-line measurement of feature dimensions during electroforming

Mandakranta Ghosh[1], XU Yang[2], Sergey Loginov[3], Marco Valenti[4], Sheng Zhou[5] and Ehsan Barati[1]

[1] University of Twente, Enschede, The Netherlands
[2] Zernike Institute for Advanced Materials, Groningen, The Netherlands
[3] University of Utrecht, Utrecht, The Netherlands
[4] AMOLF, Amsterdam, The Netherlands
[5] Vrije Universiteit Amsterdam, Amsterdam, The Netherlands

Academic supervision
Prof. dr. M.T.M. Koper, Universiteit Leiden, Leiden, The Netherlands

Company: Veco B.V., Eerbeek, The Netherlands
Contact person: Dr. Ir. Ahmad Harbiye

1. Description of company case

Veco, a leading technology company produces high precision metal parts to manufacture micro sieves which are used for filtration purposes as well as for inject printing, atomizing and nebulizing. These micro sieves are prepared by electroforming process. First, the substrate is patterned with photoresists (PR) where pores need to be created. The patterned substrate is then placed in an electrolyte bath. The target material is deposited continuously by electroforming and is allowed to deposit over the resist spots until the desired pore size is achieved as shown in figure 1. During this process, trumpet-shape holes are formed at the bath side and well-defined sharp edges are formed at the mandrel side.

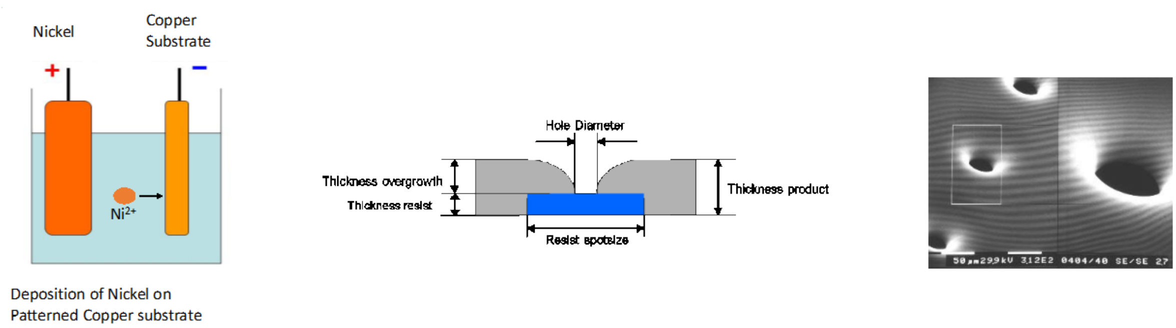

Figure 1: Process of Electroforming and creation of holes.

The size of the pores is determined by the thickness of the overgrowth, resist spot size and the thickness of the resist. Resist thickness and the spot size are well defined but the thickness of the overgrowth is defined by the total charge during deposition. This gives the amount of the target material deposited during electroforming which in turn, gives an estimate of overgrowth thickness. This estimation is highly dependent on the process conditions and influences the control over the pore size. Currently, there is no in-situ method to estimate the thickness of the overgrowth directly in order to measure the pore size accurately. This problem results in high accurate process control to minimize differences on hole sizes from plate to plate and within one plate. Veco wants the team to come up with a solution of in situ measurement of the thickness of the deposited layer to accurately control the pore size of the micro sieves.

2. Solution(s)

To measure the thickness of the deposited layer in situ, we need more than just the charge information. To address the problem our team came up with some solutions after brain storming a lot of ideas. One sets of solutions do not require any change in the substrate and another solution requires a slight modification of the substrate.

a) Solution without modifying the existing substrate:

The proposed measurements which do not require any change in the substrate are, in situ monitoring of nickel layer thickness with interferometer and electrochemical impedance spectroscopy measurements.

- **In-situ monitoring of Ni layer thickness with interferometer:**

In this process we estimated the thickness of the deposited layer with the help of an optical fiber interferometer [1]. Interferometer is a widely used technique to accurately determine nanometer to micrometer scale displacement. Here we adapt it to detect the thickness of deposition layer as shown in figure 2. Light beam emitted from the laser source is transmitted through an optical fiber and reflected by both the fiber tip surface and the substrate surface. The reflected beams interference with each other due to optical path difference and are detected by the photo-detector. The changes of the photodetector signal provide information about the changes in the substrate surface.

In our experiment, a single mode optical fiber (with a diameter of 125 um) is fixed and pointed to the substrate surface with a gap around 500 μm**.** When the deposited layer is growing on the substrate surface with time, the photo-detector signal is also collected over time. The experimental set up is shown in figure 3.

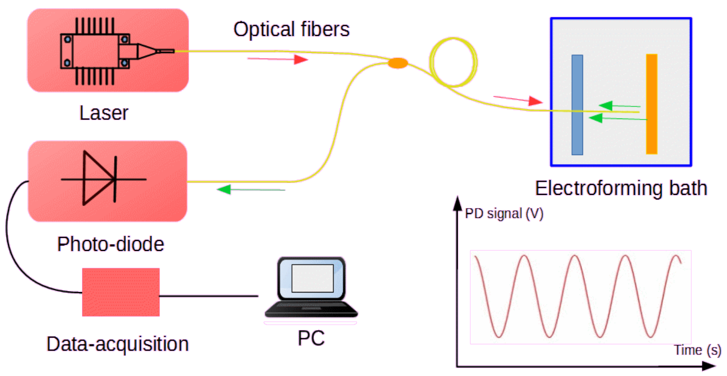

Figure 2: Schematic diagram of the experimental setup for coating thickness monitoring during electroforming process.

Figure 3: Experimental set-up. Left picture is without electrolyte, right picture is with the green electrolyte solution. The yellow wire is the optical fiber.

The substrate is taken out of the electroforming bath three times to measure the pore size during the experiment. The microscopic images of the substrate without treatment and during the pore size measurements are shown in figure 4.

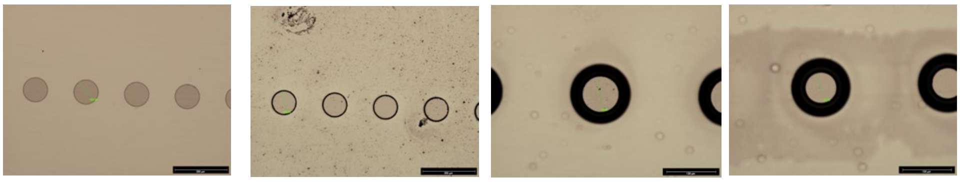

Figure 4: Images of the pore and the deposited layer with increasing time (from left to right).

Moreover, the number of interference signal sine wave periods with time are obtained from interferometer. In Figure 5 the hole sizes are plotted against the number of interference signal periods. The thickness of the deposited layer is estimated from the number of interference periods and that is also plotted against the hole size. This result proved linear relation between the number of interference signal periods and the coating thickness, as well as supported the common knowledge that the hole size is linearly related to the coating thickness (see figure 5).

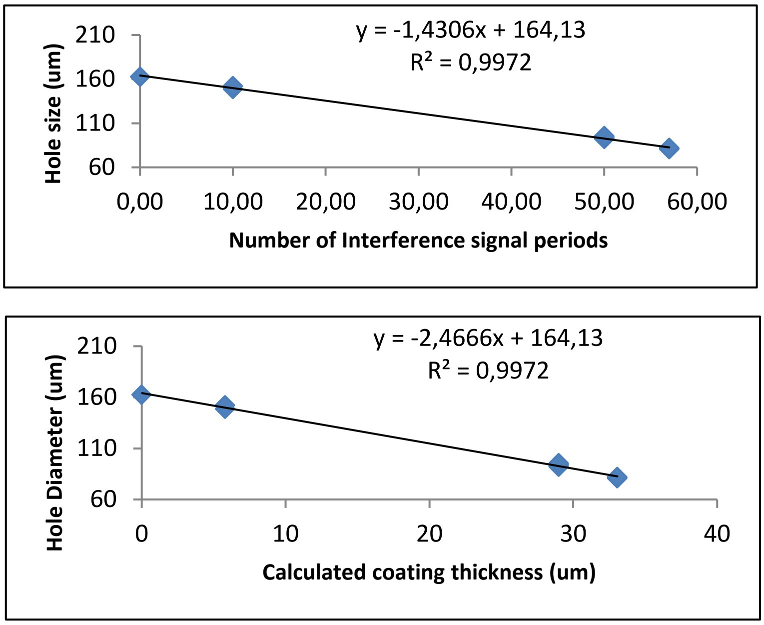

Figure 5: Hole diameter plotted against number of interference signal period s and the calculated coating thickness.

- **Electrochemical Impedance Spectroscopy:**

Another promising method which doesn't require any change of the substrate material or the standard process is Electrochemical Impedance Spectroscopy (EIS) [2]. In this method, a small AC perturbation is applied to the existing DC voltage. The current and voltage have a phase difference as shown in figure 6.

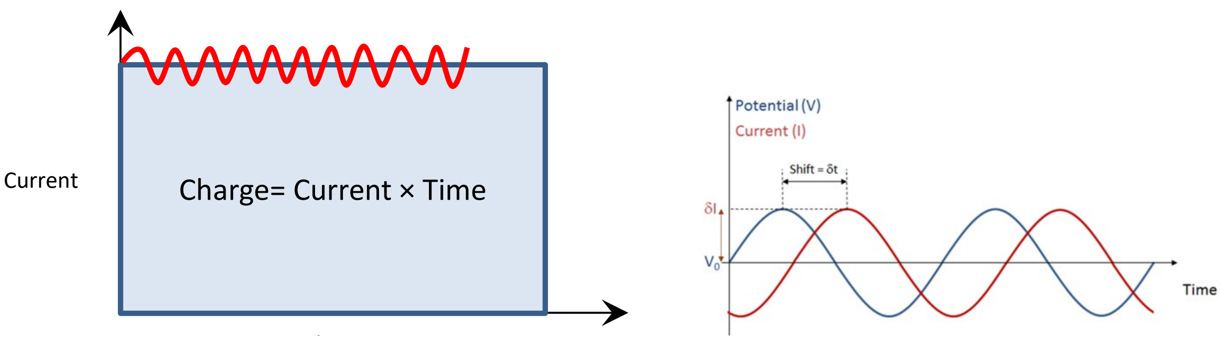

Figure 6: Small ac perturbation (red) on top of dc (left image). AC Voltage and Current vs.Time (right image).

A Nyquist plot, showing how the imaginary part of the impedance varies over the real part, can be obtained from the gained Electrical Impedance Spectroscopy (EIS) data. The data can then be processed by fitting the EIS data to the theoretical impedance of an equivalent circuit and can be illustrated in the form of a Nyquist plot. This equivalent circuit consists of individual elements representing the setup. Because the theoretical impedance of equivalent circuits can be described by equations dependent on the frequency and these specific elements of the circuit, fitting the experimental data to such a circuit results in a good description of the impedance of the setup. An example of a Nyquist plot is shown in Figure 7.

In the beginning of the electroforming process, when the photoresist layer is not coated yet there is an initial value of capacitance due to the photoresist layer. This value appears in the phase shift data. Once the deposition begins on the photoresist, one can observe a phase shift due to the change in capacitance due to the deposited material. We performed calculations for different coverage of insulator, which shows a clear evidence of phase shift at different coverages (10%, 1% and complete overgrowth). The result has been shown in Figure 8. In this method, by in-situ monitoring of the phase shift from the impedance data we will understand how much material is deposited on top of the photoresists.

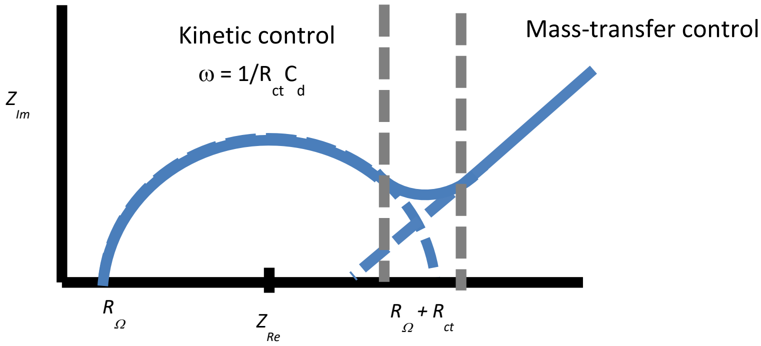

Figure 7: A standard Nyquist plot from impedance spectroscopy.

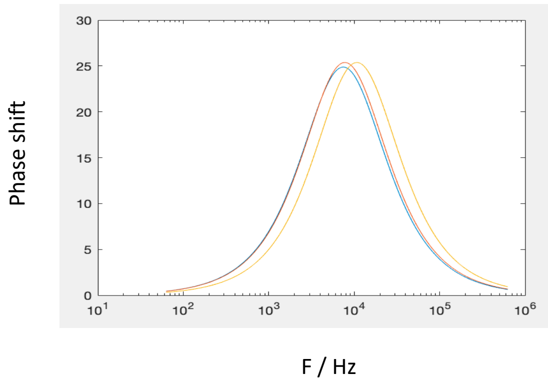

Figure 8: Phase shift at different coverage of photo resist. Yellow, red, blue line indicates 10%, 1% coverage with insulator and after overgrowth respectively.

One of the simple solutions to measure the hole size during electroforming of the patterned substrate is to do direct imaging. But the biggest problem in this case is the fact that a camera cannot be inserted into the electrolyte solution. The direct imaging can be done by a slight modification of the substrate material. We can use a transparent substrate like glass and coat it with a thin conducting layer. Then the regular process of pattering the substrate with PR can be done. We can use one of the glass walls of the electrolyte-containing reservoir as our substrate which is detachable or a glass substrate can be placed very close to the reservoir wall. In this way we can place a camera just outside wall of the electrolyte-containing reservoir so that the camera is not damaged by the electrolyte solution. A schematic diagram of the set-up is shown in figure 9.

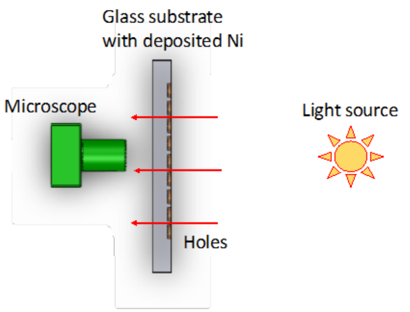

Figure 9: Schematic diagram *of the experimental set-up.*

We simulated the entire idea by imaging micro sieves placed it in front of a thick glass door at the workshop venue. We were provided with micro sieves of diameters of 20, 28, 37 and 50 m as shown in the figure 10. We first created a dark room environment and then placed the micro sieves in close contact with the thick glass door and imaged them behind the glass door. The illumination and imaging conditions were kept constant throughout the experiment.

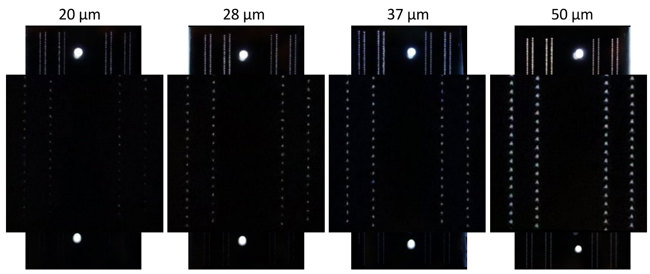

Figure 10: Micro sieves of different diameters. The middle area shows the zoomed images of each plates.

After imaging the micro sieves, we extracted the data by taking the intensity profile across the diameter of each sieve. The intensity profile shows Gaussian distribution. The data is fitted with Gaussian distribution curve as shown in figure 11. Both the fitted Gaussian width and the square root of the fitted height for each hole diameter is plotted against the hole diameter, which shows that they are linearly dependent, as shown in figure 12. This implies that from the intensity data, one can clearly get a direct estimate of the hole size during deposition at the expense of a small modification of the substrate.

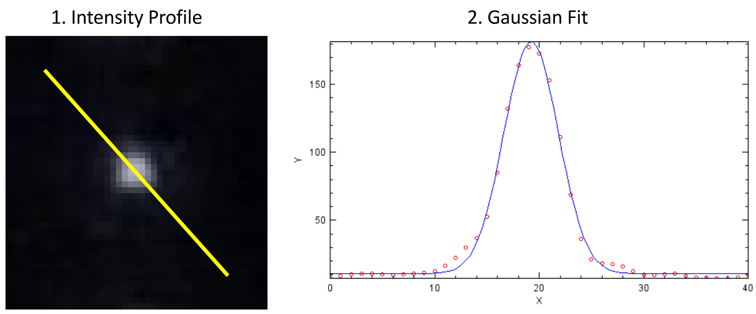

Figure 11: Data extraction from the intensity profile and the gaussian fit of the extracted data.

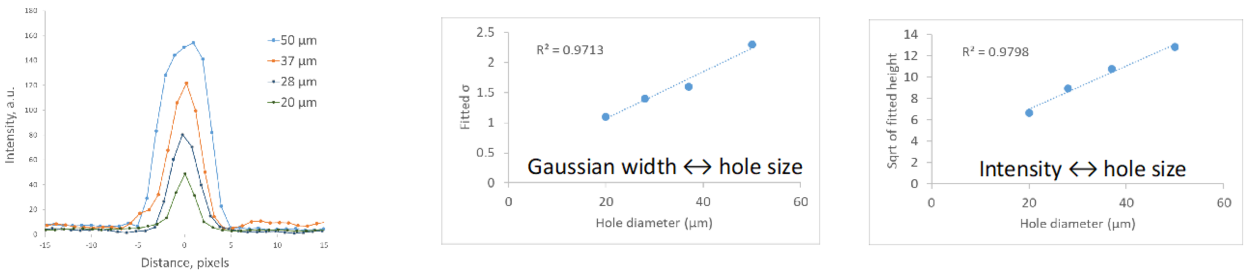

Figure 12: The fitted intensity profile for different hole sizes and the fitted intensity parameters vs. hole diameter.

The advantages of the direct imaging method are that, along with the size we also get information about the shape of the pore. The high signal to noise ratio can be utilized for automated image processing. This method also provides control over both single and multiple pore size. The equipment is simple and few LEDs will be enough to get the data. To make this method even more efficient and compact, a CCD chip placed directly behind the glass substrate is a good alternative. The CCD chip can be stuck to the glass plate by air suction and the hole-size information obtained by pinhole diffraction. Important to realize, diffraction patterns provide little information on the fine structures at the hole edges, which is nonetheless not essential for the determination of hole sizes.

- **Controlling the pore size variation in the same plate:**

Once we solved the issue with the in-situ measurements of the overgrowth layer, we were interested to find out how to solve the of pore size variation in the same plate. We think that the fundamental reason of variation of pore sizes in the same plate is different amount of deposition of material on the substrate as the process conditions can vary at different regions of the plate. One of the factors controlling the deposition rate is temperature. Local temperature controls the local deposition rate. The electroforming of nickel is diffusion limited. The current density is dependent on the diffusion coefficient which consequently is a function of temperature as given by equation 1 and 2 [3].

Current density: $$j = D(T) \times \frac{nF}{\delta} C_{Ni} \qquad (1)$$

Diffusion Coefficient: $$D(T) = T \times \lambda(T) \times \frac{R}{nF^2} \qquad (2)$$

Where:

T= Temperature
R= Molar gas constant
λ= Molar Conductivity of Nickel ions
δ= Diffusion layer thickness
n= Total charge liberated by reaction
F= Faraday constant
C_{Ni}= Concentration of Ni ions at the bulk

From the production conditions, we know that the applied current density is 0.09A/cm^2 and the temperature is 50^{o}C. From equation 1 and 2 we calculated the deposition rate at different temperatures varied from 40^{o}C to 60^{o}C. The deposition rate at different temperature, normalized with the deposition rate at 50^{o}C is plotted against temperature as shown in figure 13. From figure 13 we see that the deposition rate varies 20% with a variation of only 10^{o}C temperature.

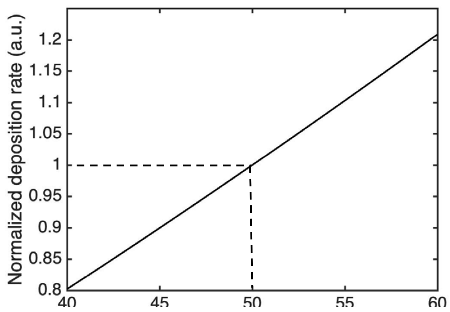

Figure 13: The variation of Normalized deposition rate with temperature

The variation of local temperature can be controlled by thermoelectric cooler chips which are commercially available from 8x8 mm^2 to 30x8 mm^2 size. In this way, the variation in the local temperature can be controlled which will control the local deposition rate and thereby evenly sized pores in the entire substrate.

3. Conclusion and Outlook:

To control the size of the holes during electroforming process we proposed and tested two sets of solutions: with and without any change in the substrate. The former is highly desired in which, without major modification of the substrate, we can monitor the surface area growth in-situ by applying an AC perturbation over the DC voltage and collect the phase information. Then, using additional interferometer one can directly and precisely monitor the film thickness. As for the latter, with slight modification of the substrate, incorporating a glass substrate and an image sensor one can also directly and precisely monitor the size of individual holes and regional averages. Moreover, local temperature adjustments can be carried out to control the hole-size variation within the same plate. In summary, the obtained results offer a clear, straightforward, and technically feasible solution to this case.

4. References

[1] Milewska, D., Karpienko, K. and Jędrzejewska-Szczerska, M., 2016. Application of thin diamond films in low-coherence fiber-optic Fabry Pérot displacement sensor. Diamond and Related Materials, 64, pp.169-176.

[2] Journal of Applied Electrochemistry **30**: 1125-1132, 2000., Kluwer Academic Publishers, Netherlands,2000

[3] Petr Vanyśek, CRCHandbook of Chemistry and Physics; CRC Press: Boca Raton, FL, 2005.

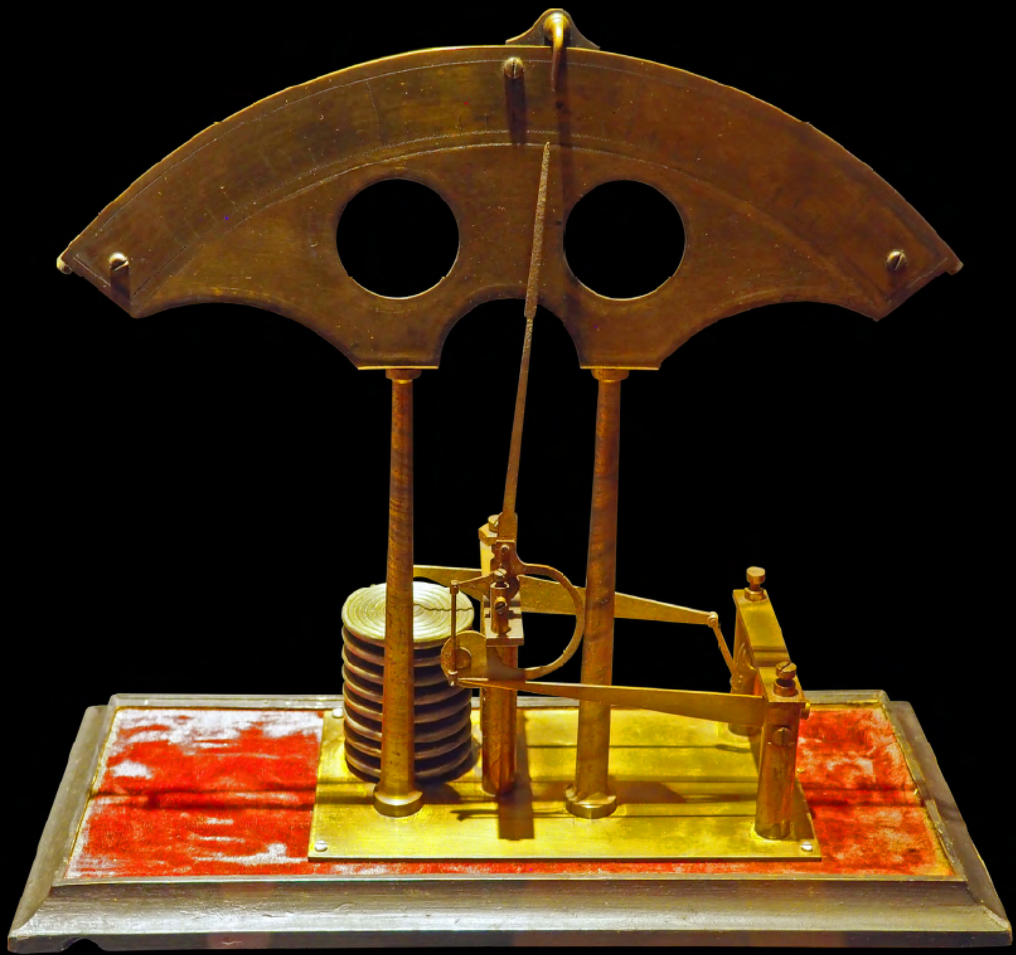

NWO

Lorentz center